APPLICATION OF HEAVY ION BEAMS TO CONDENSED MATTER STUDIES

H.-E.Mahnke

Hahn-Meitner-Institut Berlin GmbH
Bereich Kern- und Strahlenphysik
D-1000 Berlin 39, W.Germany

ABSTRACT

The use of heavy ion beams in condensed matter studies and materials science is overviewed by discussing selected examples. The examples range from studies with isolated nuclear probes in solids to investigate atomic and electronic structures on a local scale, to materials modification by implantation, studies on ion-solid interaction, and materials analysis with ion-beam techniques.

INTRODUCTION

Heavy ion accelerators, such as cyclotrons as well as other accelerator combinations, are typically designed and used as research tools in the field of nuclear physics. So far there is only a small number of facilities with broader programs for applications of heavy ion beams to condensed matter studies. At VICKSI, an increasing fraction, at present a third, of the beam time is used for the investigation of problems in solid state physics. And at this Conference the program for a dedicated facility, the Advanced Radiation Technology (ART) project in JAERI has been presented by R.Tanaka [1]. Typical heavy ion beams used cover the whole range in ion mass, and their energies range from 0.5 to 5 MeV/u. In a few studies even higher energies are being used, e.g. at GANIL (CIRIL) and at GSI [2],[3].

In the following survey two major categories of materials studies will be described for which heavy ion beams are being employed:

(i) production and implantation of nuclear probes in solids by nuclear reactions, combined in a natural way with nuclear techniques such as Mössbauer spectroscopy, perturbed angular correlation (PAC) and perturbed angular distribution (PAD), and β-NMR; and

(ii) materials modification and analysis, deep implantation and the investigation of ion-solid interaction in combination with ion-beam techniques such as Rutherford backscattering spectroscopy (RBS), elastic recoil detection analysis (ERDA), nuclear reaction analysis (NRA) as well as measurements of bulk properties, e.g. resistivity.

A few examples out of both categories have been chosen to illustrate the scope of applications in solid state physics and materials studies. They range from simple irradiations of various materials to complicated and sophisticated setups with electronics as commonly used in nuclear physics experiments.

NUCLEAR PROBES IN SOLIDS

The investigation of the condensed matter with nuclear probes takes advantage of the high sensitivity with which radiating excited (or unstable) nuclei are detected. Because of that high sensitivity the total number of radiation emitting nuclei necessary in a typical experiment lies between 10^7 to 10^{11} nuclei only. When transformed into a concentration an extreme dilution is self-evident: under the recoil-implantation conditions as illustrated in Fig.1 concentrations as low as 10^{10} to 10^{14} nuclei/cm^3 (less than 10^{-2} ppma) are easily realized.

The information about the solid is obtained via the hyperfine interaction of the nuclear probes, which acts on a local scale and yields insight into the local structure of the material of interest. The hyperfine interaction can always be factorized into a nuclear parameter such as the nuclear radius $\langle r^2\rangle$, nuclear magnetic moment μ, and nuclear electric quadrupole moment Q, and the corresponding atomic parameter, influenced and altered by the solid state environment, the electron density $|\Psi(0)|^2$, the magnetic field B(0), and the electric field gradient $\partial^2V/\partial z^2$. Via such interactions nuclear probes measure local electronic structures, e.g. local magnetism as well as local lattice struc-

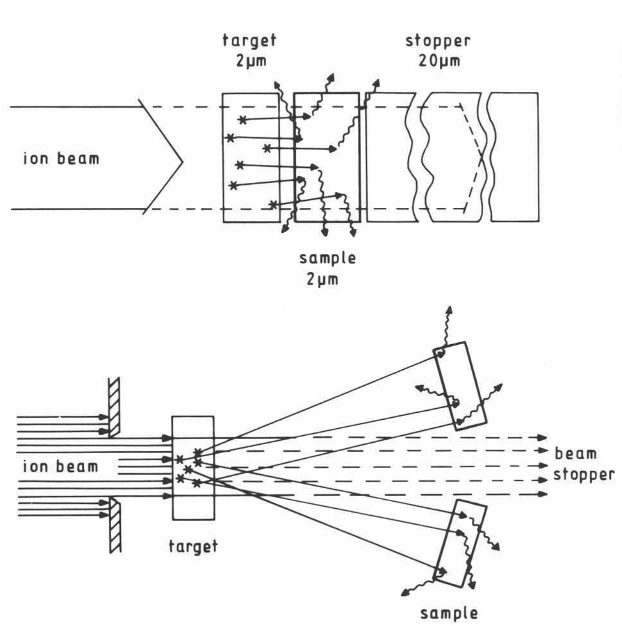

Fig.1: Sample preparation schemes for recoil-implantation: In the arrangement sketched in the upper part the primary ion beam passes through the sample, in the arrangement shown in the lower part passage of primary ions through the sample is avoided.

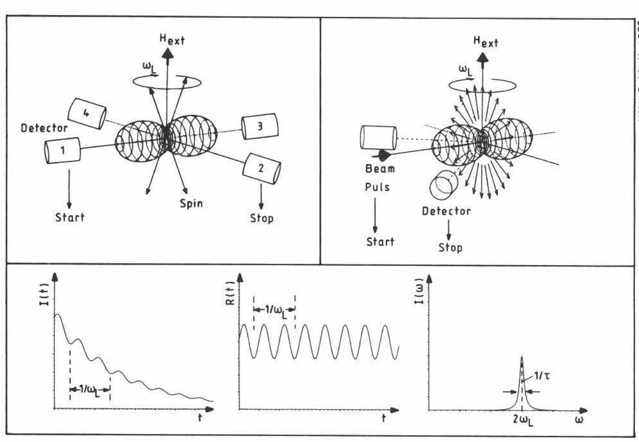

Fig.2: Principle of PAC and PAD: Either by a nuclear reaction (PAD, top right) or by detecting a preceding transition in correlation (PAC, top left), an aligned ensemble of radiating nuclei is produced. An anisotropic emission results for the radiation. Changing spin alignment with time yields time dependent changes of the emission pattern. For a spin precession in a magnetic field as sketched, a sine-like modulation is observed superimposed to the exponentially decaying intensity as observed in a single detector (left), with the exponential decay divided out by properly combining the intensity spectra of several detectors (center), or as Fourier-transforms (right).

tures, e.g. point defects. The nuclear probe may be the excited nucleus of a constituent as well as of an impurity atom within the solid. Static as well as dynamic processes including the microscopy of diffusion are studied.

As experimental methods the Mössbauer spectroscopy, perturbed angular correlation and distribution, and radiative detected nuclear magnetic resonance are being used, which all employ isomeric or unstable nuclear states with lifetimes between nanoseconds and milliseconds. The hyperfine interactions are determined either as energy differences directly as in MS, or as absorbed radiofrequency in radiative detected NMR, or as modulation frequencies in the time-dependent γ-ray intensity in PAC or PAD, see Fig.2 [4)].

The essential feature in this context is the use of heavy ion nuclear reactions for the production and the implantation of nuclear probes. Two somewhat different schemes are being followed as sketched in Fig.1. The target, in which the reaction takes place, the sample, and a stopper, which may also be the thicker part of the sample, are mounted as a sandwich. Such an arrangement is necessary for the in-beam PAD technique, where the produced nuclear probes recoil out of the target foil directly into the sample (a gap in-between should be avoided for most cases). As a consequence the primary ion beam always passes through the sample. For in-beam Mössbauer spectroscopy [5)] as well as for the production of radioactive sources for off-line experiments (PAC or MS) direct beam passage can be avoided by separating target and sample taking advantage of the different angles of recoil products and primary ion beam.

Two examples illustrate the use of nuclear probes for local information on solids.

The Local Moment of Isolated Ni Ions in Alkali Metals

When an ion is embedded into a metal it usually looses most of its ionic character by the interaction of its outer electrons with the neighboring host ions and the conduction electrons. In a recent study W.-D.Zeitz et al. [6)] investigated the formation and the behavior of local magnetic moments of isolated Ni atoms in alkali metal hosts. Isomeric ^{63}Ni nuclei were produced via the ^{48}Ca(^{18}O,3n) using a pulsed ^{18}O beam of 45 MeV provided by VICKSI. The probe nuclei were recoiled out of the target foil into alkali metal hosts at different temperatures and the local magnetic susceptibility was determined by PAD.

Their observations are summarized with the illustration given in Fig.3. The local magnetism at the Ni ion in the heavy alkali elements Cs, Rb, and K follows a Curie-like paramagnetic behavior. The explanation requires the existence of monovalent Ni ions with spin-orbit coupled 3d^9 configurations. The simultaneously measured spin fluctuation rates indicate a very weak hybridization of the Ni ions in the Cs, Rb, or K lattice. A comparison of the ionic radii of the alkali ions with the radius of Ni in different ionic states gives the base for the interpretation: there is only little interaction of the highly undersized Ni ion with the neighboring K, Rb, or Cs alkali ions (only small sd hybridization), and fully localized 3d electrons are observed.

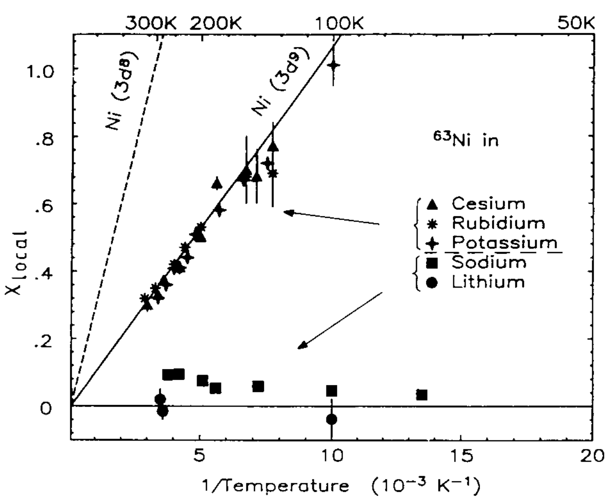

Fig.3: Local magnetic susceptibility of Ni in alkali metals as derived from the measured modulation frequencies in an externally applied magnetic field H_{ext}, $H_{observed}=(1+\chi_{loc})\cdot H_{ext}$. For the heavy alkali elements K, Rb, and Cs a fully localized $3d^9$ electronic configuration is observed.

While the occurrance of fully localized magnetic configurations is well established for isolated 4f elements (the rare earths) in various metals, it was found for the 3d elements Fe and Ni (the example given here) and, in the meantime for 4d elements, too [7], only with the help of recoil implantation following heavy ion reactions, since such systems cannot be alloyed.

Neutrino-Recoil-Induced Frenkel Pairs

The properties of any material are often dependent on the nature and concentration of imperfections. In semiconductors structural defects are strongly linked with electronic defects, and an understanding of their microscopic nature is highly desired. Nuclear techniques using nuclear probes do not only help to reveal their microscopic nature, taking advantage of well-known kinematics in nuclear decays nuclear techniques are also used to produce well-defined isolated point defects under controlled conditions.

Using the neutrino-recoil effect in electron capture decays H.Metzner and R.Sielemann found a way to produce and investigate single isolated Frenkel pairs (vacancy and interstitial atom). First studied in metals like copper [8] this production scheme is now applied to semiconductors, too. The authors use the standard PAC nucleus ^{111}Cd, but not via the mother activity ^{111}In directly, but rather the precursor ^{111}Sn is taken. The ^{111}Sn nuclei are produced and recoil-implanted with a heavy ion nuclear reaction using an arrangement as sketched in Fig.1. At VICKSI a 100-MeV ^{22}Ne beam is used for the ^{93}Nb(^{22}Ne,p3n)^{111}Sn reaction. The main decay-branch of ^{111}Sn is an electron capture decay ($T_{1/2}$= 35 min) with the emission of a neutrino with well-defined high energy of 2.5 MeV to ^{111}In which is thereby given a well-defined recoil energy of approximately 29 eV. ^{111}In is the 'mother-activity' ($T_{1/2}$=2.8 d) for the standard PAC nucleus ^{111}Cd (likewise ^{57}Co is the mother-activity for the often used ^{57}Fe in Mössbauer spectroscopy). The recoil energy provided by the electron capture decay of the ^{111}In to the ^{111}Cd, the actual probing atom, is less than 1 eV, much too small to change the situation. The halflife of the precursor ^{111}Sn is just long enough to allow for sample treatment like annealing in order to start the experiment with a well-prepared sample in which the ^{111}Sn nuclei occupy a substitutional, undisturbed lattice position. With the neutrino emission the resultant ^{111}In nucleus is given a recoil energy sufficient to

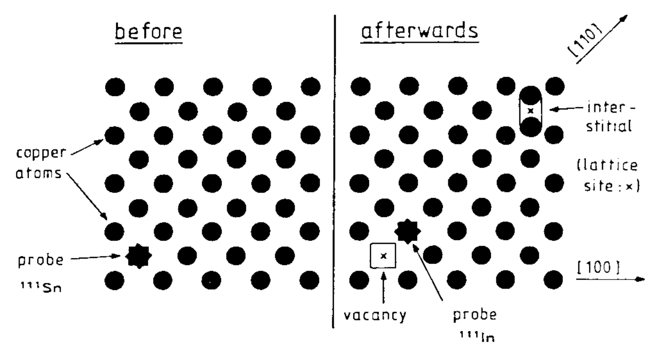

Fig.4: Microscopic picture of the neutrino-recoil effect in the decay of the probe ^{111}Sn (before) to ^{111}In (afterwards) within a fcc-type crystal lattice (copper).

move to the nearest neighbor position by kicking out the lattice atom and leaving behind a monovacancy. The replacement collision sequence initiated by the recoiling In as the primary knock-on atom leads to a monointerstitial at some distance (Fig.4). The vacancy neighboring the PAC nucleus ^{111}In results in a noncubic symmetry detected by the nuclear quadrupole interaction as a modulation in the PAC time spectrum (Fig.5). Determining the amplitude of the modulation with increasing annealing temperature the annihilation of the vacancy is observed, first by the migration of their own interstitial atom back to the vacancy (recombination) and later at higher annealing temperatures by detrapping from the In.

The production of isolated Frenkel pairs by the neutrino recoil energy is, of course, only possible when certain energy conditions are fulfilled: The recoil energy must be larger than the threshold energy for Frenkel pair production, but not too large, otherwise more complicated defect structures will be formed. While isolated Frenkel pairs have been observed for copper and other metals, it was not found for e.g. gold, a finding consistent with a too high threshold energy. The results for metals already illustrate that the neutrino-recoil effect is a rather useful approach on a microscopic scale to the energetics of the formation of isotated Frenkel pairs in different materials. First results for semiconductors further on indicate a dependence on the Fermi level which has to be exploited.

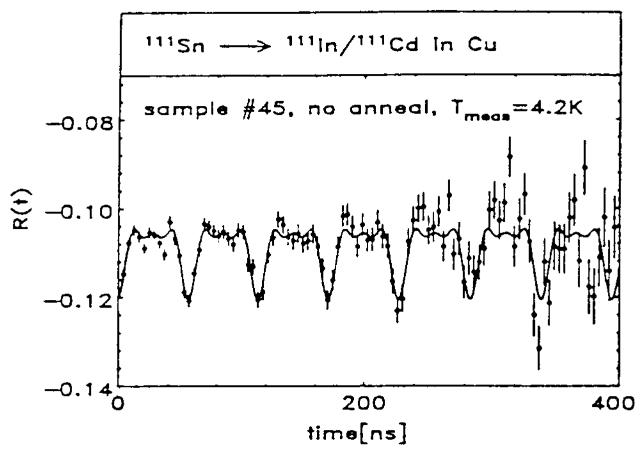

Fig.5: PAC-signal of the monovacancy as nearest neighbor to the ^{111}In probe following the neutrino recoil.

MATERIALS MODIFICATION AND ANALYSIS

In this category of use of heavy ions for materials studies, the macroscopic behavior and properties are the major points of interest. The underlying microscopic mechanisms, however, have to be well understood. They are therefore subject of own research programs in many cases.

In the following three examples have been chosen to give an idea about the scope of the use of heavy ions in this part of the field.

High-Energy (-Deep-) Implantation of Boron in Silicon

In semiconductor technology the terminology of "high energy" is typically used for ions with energies between 0.5 and 5 MeV. In the example discussed here the term high energy comes closer to the understanding of the accelerator (better cyclotron) community, namely higher than 50 MeV. The elements often used as dopants in silicon are among the species of ions produced at the VICKSI accelerator with currents allowing device fabrication within reasonable irradiation times.

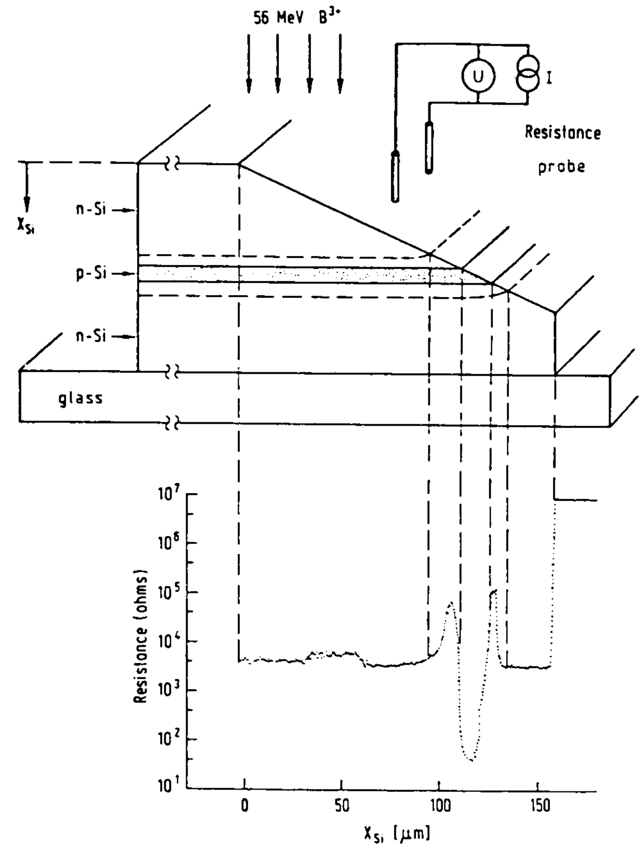

Fig.6: Implantation profile of deeply implanted 56-MeV ^{11}B in silicon as determined by the spreading resistance measurements along a bevel of the Si wafer following annealing at 1100°C (after [10]).

K.-G.Oppermann and W.R.Fahrner [9] have used a 50-MeV ^{11}B beam for the production of a thyristor by deep implantation into silicon. At this energy the implantation depth in silicon is approximately 100 μm. The procedure has been studied earlier [10] with respect to destruction of the semiconductor, amorphization, annealing of damage, and the implantation profile with promising results. An example for the determination of the implantation profile using the spreading resistance technique along a bevel of the silicon wafers is shown in Fig.6. For the actual diodes the doping profiles were determined in the same way (Fig.7). Structures were studied for various implantation doses. E.g. diodes without deep implantation had a maximum blocking voltage of 900 V, with the buried B layer at a dose of 10^{13} cm^{-2} the blocking voltage had increased to 2000 V. Diodes with the highest dose of $2{\cdot}10^{14}$ cm^{-2} showed typical thyristor-like characteristics, forward breakdown voltage etc.

The devices produced and studied so far at VICKSI demonstrated two advantages: (i) excessive drive-in temperatures can be avoided in the process after the implantation, thereby reducing the broadening of the buried layer, (ii) deep structures are easily produced. Two possible disadvantages turned out to be of minor importance: (i) the radioactivity is short-lived, and (ii) the defect density is largely reduced due to annealing during the further processing steps without any specific annealing steps. As a result the creation of structures buried within the bulk material by using high-energy heavy ion beams is a promising field for applications.

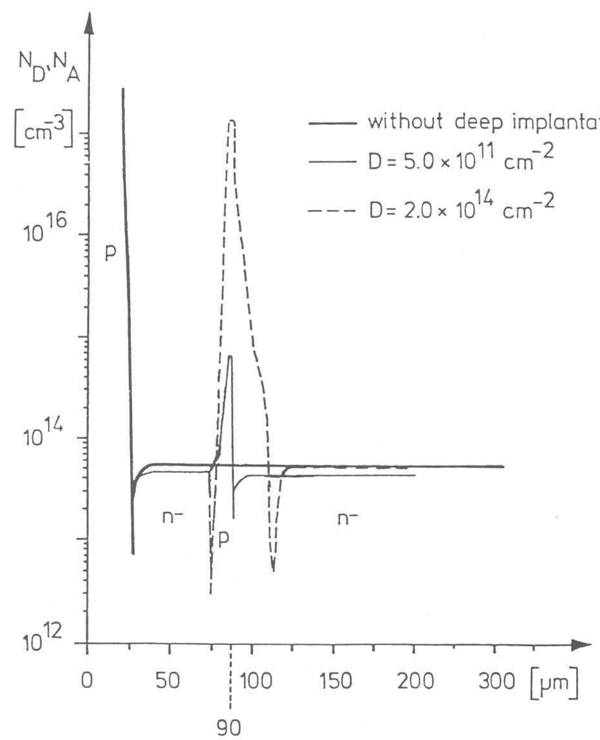

Fig.7: Doping profiles of Si diodes with a deeply implanted layer of ^{11}B (after [9]).

Ion-Beam-Induced Plastic Flow of Glassy Material

With the increasing use of high-energy heavy ions in device fabrications (as in the preceding section), microstructures [2], etc. a deep understanding of the ion-solid interaction is highly needed. As discussed by B.E.Fischer [2] a single heavy ion brings such a large local energy density into the solid along its path that atomic rearrangements occur leading to etchable tracks in various classes of material. In this context S.Klaumünzer et al. [11] observed that metallic glasses undergo macroscopic shape changes when irradiated with high-energy heavy ions at temperatures well below the glass transition temperature. Above an incubation dose metallic glasses grow in the directions perpendicular to the direction of the beam (the energy of which is high enough so that the beam passes through the sample) while shrinkage is found in the direction parallel to the beam. The density remains nearly constant. Fig.8 gives an example. At a fluence of $1.7 \cdot 10^{13}$ ions/cm^2 of a 360-MeV Xe beam the length and width of the sample shown has changed by 15 %. The authors could establish a linear dependence of the dimensional changes on the fluence in the form

$$\Delta l/l_o = \Delta b/b_o = A \cdot (\Phi t - B)$$

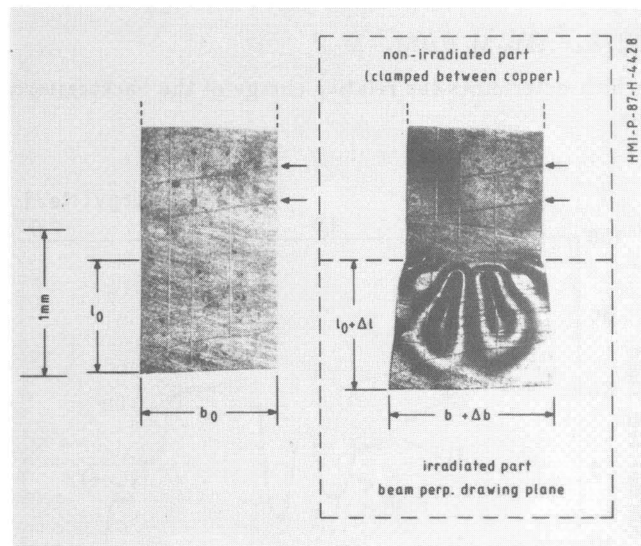

Fig.8: Plastic deformation due to ion-beam irradiation: (left) Part of the unirradiated sample of $Co_{75}Si_{15}B_{10}$ glass. The arrows mark two scratches to facilitate the dimensional measurements; (right) the same sample with the lower part homogeneously irradiated with 360-MeV Xe ions at a temperature below 50K, the ions traverse the sample.

The experiments so far are summarized in three major observations:

(i) ion-beam induced growth is a universal behavior for a wide class of glasses, conducting (metal-metalloid-like glasses), semiconducting (hydrogenated amorphous silicon a-Si:H), and nonconducting (quartz) glasses;

(ii) no growth is found for crystalline material;

(iii) the growth rate A is directly linked to the electronic stopping power.

These observations led the authors to the following model-like interpretation: Along the ions path ionization takes place through electronic stopping, the then charged cylinder explodes due to Coulomb forces (Coulomb explosion), triggering shear transitions and leading to atomic rearrangements. When there is free volume as in amorphous material then no relaxation back to the original configurations occurs, and the plastic deformation is found.

Composition of High-Temperature Superconducting Films

In materials research, especially in the preparation of thin films or layered structures, ion beams are becoming a standard tool in the materials analysis. One technique most commonly used is the Rutherford backscattering spectroscopy. The technique is based on simple relations between the mass M_1 and energy E_0 of the incoming ion (with Z_1) and its energy E_1 when scattered to an angle Θ by a sample atom with mass M_2 (and Z_2). Its sensitivity to different elements in analyzing compositions of various materials results from the so-called kinematic factor

$$E_1/E_0 = (M_2 - M_1)^2/(M_1 + M_2)^2$$

which determines the relative energy of the backscattered ion.

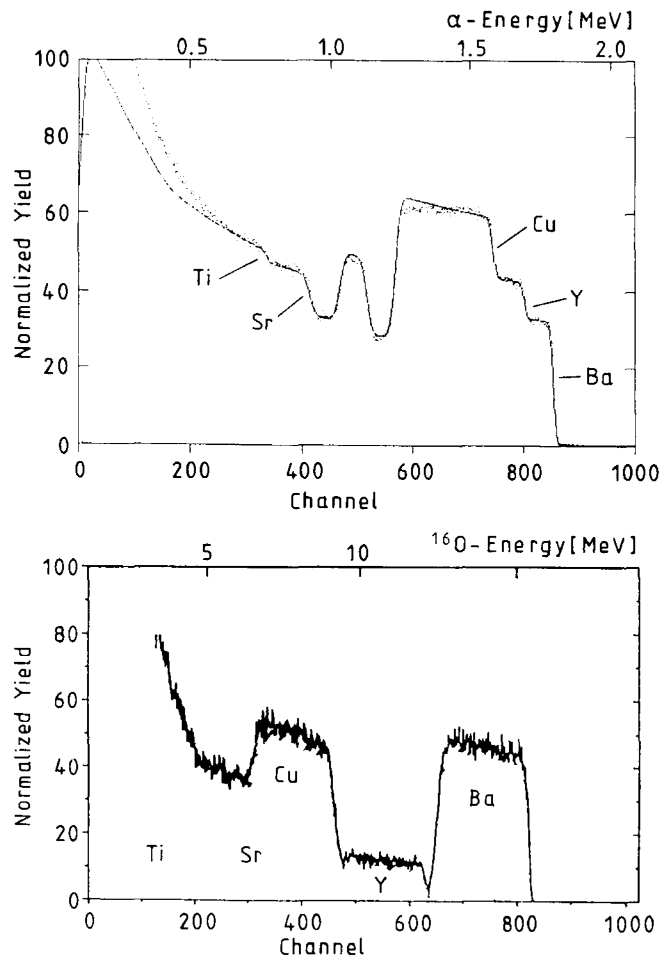

Fig.9: Rutherford backscattering spectrum of α-particles on an epitaxially deposited $YBa_2Cu_3O_7$ film (about 700 nm thick) on $SrTiO_3$. Top: Sputtered film (J.Erxmeyer et al. [12]) analyzed with 2-MeV α-particles; bottom: film after laser ablation (W.Schindler and B.Roas [13]) analyzed with 25-MeV ^{16}O ions from the University of Erlangen tandem.

The most widely used particle in RBS is the α-particle. In the research on high-temperature superconducting films epitaxially deposited $YBa_2Cu_3O_7$-films have to be analyzed for their constitutional composition and homogeneity. In Fig.9 the RBS analysis of a film with 2-MeV α-particles is compared with an analysis using 25-MeV ^{16}O ions from a tandem accelerator. The higher sensitivity of the heavy ion in determining the composition of the three metallic constituents is clearly illustrated.

As is obvious from the example shown RBS cannot be used to analyze all possible elements. Other nuclear techniques are at hand for light elements. In the case hydrogen the nuclear reaction analysis using the $H(^{15}N,^{12}C)\alpha$ reaction at resonance is the most common technique. A variant of the RBS, the elastic recoil detection analysis, may also be a useful alternative in determining light elements.

ACKNOWLEDGEMENT

With most of the examples discussed in this overview I am not directly connected. I am therefore very much indebted to many friends and colleagues for letting me present examples of their research projects. Special thanks go to D.Bräunig, J.Erxmeyer, S.Klaumünzer, H.Metzner, A.Weidinger, W.-D.Zeitz, and K.Ziegler at the Hahn-Meitner-Institut in Berlin and to B.Roas, G.Saemann-Ischenko, and W.Schindler at the Phys. Inst. Universität Erlangen who provided me with the 25-MeV ^{16}O RBS example.

REFERENCES

1) Tanaka,R., Arakawa,K., Yokota,W., Nakamura,Y., Kamiya,T., Fukuda,M., Agematsu,T., Maruyama,M., "JAERI AVF cyclotron for research of advanced radiation technology", presented at this Conference

2) Fischer,B.E., "Production of microstructures by heavy ions", presented at this Conference

3) Symposium on 'Swift Heavy Ions in Matter' (SHIM), Caen, May 1989

4) Mahnke,H.-E., "Introduction to PAC/PAD", Proc. Intern. Conf. on Nuclear Methods in Magnetism, München 1988, in press in Hyp. Int.

5) Sielemann,R., "The study of point defects in metals by Perturbed Angular Correlation and the Mössbauer effect", Materials Science Forum 15-18, 25 (1987)

6) Kowallik,R., Bertschat,H.H., Biedermann,K., Haas,H., Müller,W., Spellmeyer,B., Zeitz,W.-D., "Observation of a fully localized $3d^9$ configuration for nickel ions in alkali metals", accepted by Phys. Rev. Lett. (1989)

7) Riegel,D., Gross,K.D., "Local magnetism in alloying and nonalloying systems", in: Nuclear Physics Application on Materials Science (E.Recknagel, J.C.Soares, eds.); Nato ASI series E Vol.144, 327 (1988)

8) Metzner,H., Sielemann,R., Butt,R., Klaumünzer,S., "Single Frenkel-pair production by neutrino recoil", Phys. Rev. Lett. 53, 290 (1984); Metzner,H., Sielemann,R., Klaumünzer,S., Hunger,E., "Production and thermal annealing of neutrino-recoil-induced Frenkel pairs in copper", Phys. Rev. B36, 9535 (1987)

9) Oppermann,K.-G., Fahrner,W.R., "Results of boron implantation into silicon diodes and metal-oxide-semiconductor gate-controlled turn-off thyristors", Materials Science and Engineering B2, 75 (1989)

10) Fahrner,W.R., Laschinski,J.R., Bräunig,D., "Application of high energy implantation in semiconductors", Nucl. Instr. and Meth. A268, 579 (1988)

11) Klaumünzer,S., Hou Ming-Dong, Schumacher,G., Li Chang-Lin, "Ion-beam-induced plastic deformation of amorphous materials", Mat. Res. Soc. Symp. Proc. 93, 21 (1987) and further ref. therein

12) Erxmeyer,J., Weidinger,A., "Herstellung dünner Y-Ba-Cu-O Filme mit Ionenstrahl-Sputtern", Verh. DPG (VI) 24, TT12.13 (1989) and private communication

13) Schindler,W., Roas,B., private communication